

Article

Land Use Sustainability: Assessment of the Dynamic Response of Typical Bedrock-Buried-Hill Earth Fissure Sites in the Su-Xi-Chang Area

Ge Cao ¹ , Yahong Deng ^{1,2,*}, Huandong Mu ³, Jiang Chang ¹, You Xuan ¹ and Dexin Niu ¹

¹ School of Geological Engineering and Geomatics, Chang'an University, Xi'an 710054, China; 2020026038@chd.edu.cn (G.C.)

² Key Laboratory of Mine Geological Hazards Mechanism and Control, Ministry of Natural Resources, Xi'an 710054, China

³ Institute of Geotechnical Engineering, Xi'an University of Technology, Xi'an 710048, China

* Correspondence: dgdyh@chd.edu.cn

Abstract: Disaster prevention and the mitigation of earth fissures is a key issue in the sustainable development of urban land. Structures directly avoiding earth fissures are not conducive to the rational planning and efficient utilization of urban construction. The Su-Xi-Chang area, which consists of the cities of Suzhou, Wuxi, and Changzhou, surrounded by Taihu Lake, has developed bedrock buried-hill earth fissures that are rare in the rest of the country. Existing research results have identified the genesis mechanisms, distribution patterns, and developmental characteristics of this type of fissure. Not only does the slow-variable activity of earth fissures cause direct damage to surface and underground structures, but in addition, when an earthquake occurs, the presence of earth fissures may cause the seismic response of the site to be altered or even strengthened, leading to unknown damage or the possible destruction of structures near the fissures. However, no studies have been conducted to assess the dynamic effects of bedrock-buried-hill earth fissure sites. Therefore, in this research, based on six typical bedrock-buried-hill-type earth fissures in the Su-Xi-Chang area, and in order to accurately reveal the dynamic amplification effect law of the earth fissure sites, systematic spectral analyses and comparisons of the microtremor signals were carried out by using the linear analysis method (Direct Fourier Transform Analysis) and the nonlinear analysis method (Hilbert–Huang Transform). The results show that bedrock-buried-hill-type earth fissures have a significant amplification effect on the dynamic response of the site; the amplification effect of bedrock-buried-hill fissure sites follows the same attenuation pattern, and the furthest range of the dynamic response on the site is about 25 m, beyond which the original seismic fortification level can be maintained; the extreme value of the amplification factor of the two sides of this type of site, as derived from the Fourier and HHT methods, is about double, and the nearest earth fissure region should be considered to have a raised seismic fortification intensity of more than double the original. The Hilbert–Huang transform method has good applicability for processing microtremor data, and nonlinear signal analysis methods can be considered comprehensive for future microtremor signal processing.

Keywords: earth fissure disaster prevention and mitigation; microtremor testing; amplification effect; spectrum analysis; sustainable development



Citation: Cao, G.; Deng, Y.; Mu, H.; Chang, J.; Xuan, Y.; Niu, D. Land Use Sustainability: Assessment of the Dynamic Response of Typical Bedrock-Buried-Hill Earth Fissure Sites in the Su-Xi-Chang Area. *Sustainability* **2024**, *16*, 3117. <https://doi.org/10.3390/su16083117>

Academic Editor: Antonio Miguel Martínez-Graña

Received: 19 January 2024

Revised: 4 April 2024

Accepted: 7 April 2024

Published: 9 April 2024



Copyright: © 2024 by the authors. Licensee MDPI, Basel, Switzerland. This article is an open access article distributed under the terms and conditions of the Creative Commons Attribution (CC BY) license (<https://creativecommons.org/licenses/by/4.0/>).

1. Introduction

Earth fissures are geological disasters that occur worldwide. It involves linear tensile cracking with a specific extension length that develops on the land surface and may be accompanied by vertical dislocation. Earthquakes and active faults, underground mining, groundwater mining, and landslides can cause earth fissures [1]. China is one of the countries most severely affected by earth fissure disasters because of the large number

and development scale of earth fissures and their wide distribution area. From 1966 to 2000, more than 6000 earth fissures were identified in China, with a cumulative length of more than 1000 km, affecting an area of more than 600,000 square kilometers. The three main areas of earth fissure development in China, namely the Fenwei Basin, the Hebei Plain, and the Su-Xi-Chang area, encompass 70% of the total number of earth fissures in China [2]. The special bedrock-buried-hill-type earth fissure is rare in China, but 25 typical bedrock-buried-hill-type earth fissures have been identified in the Su-Xi-Chang area, which is composed of the cities of Suzhou, Wuxi, and Changzhou around Taihu Lake [3]. The Su-Xi-Chang area is a prosperous metropolitan region in China, with densely built-up areas and complex traffic tunnels, and the active deformation of earth fissures has seriously impeded the high-speed development of the regional economy. In order to prevent earth fissure disasters, there has been some research into the development and distribution of bedrock-buried-hill-type earth fissures, analyzing their activity characteristics, genesis mechanisms, formation, and evolution. Static subsidence and the deformation of earth fissures have been identified as topics for study, and many consensus results have been achieved [4–9].

The various stratigraphic and topographic features of a project site often lead to specific seismic responses, which become a site-effect topic. Different studies for particular site conditions such as bedrock [10] and slopes [11] have revealed that the response patterns of irregular terrain sites in earthquakes are significantly different. Among them, earth fissures are an extremely significant engineering and geological issue, and many researchers and scholars have produced preliminary results revealing that the earth fissure site in Xi'an, China has potential dynamic amplification effects based on numerical simulations and physical model tests [12–15]. However, it is difficult for the existing results to provide a reference for the seismic fortification of earth fissure sites with special genesis types such as bedrock buried hills. Therefore, there is an urgent need to characterize the dynamic response of bedrock-buried-hill-type earth fissure sites.

Considering the randomness of earthquakes, the time-consuming observation of measured earthquake data at earth fissure sites, and the difficulty of obtaining large-scale earth fissure site monitoring data, scholars have begun to search for alternatives in assessing the seismic field effects at sites.

In 1908, Omori observed an extremely weak foundation vibration with a high-multiple-vibration measuring instrument and named it a 'microtremor' [16]. Subsequently, in the 1950s, Kanai vigorously promoted the microtremor as an evaluation method of engineering site performance [17], popularizing it in Japan. Since then, scholars have conducted a series of studies on the microtremors' sources, genetic mechanisms, and wave patterns [18–21]. However, research at this stage is mainly limited to short-period constant time microseisms below 1 s. In the 1970s, with the emergence of more high-rise buildings, the effect of deep site conditions on ground vibrations received some attention, and long-period microtremor observations of greater than 1 s were carried out. In the 1990s, Nakamura proposed a microtremor single-point spectral ratio method (H/V) [22] that once again formed a hot spot in the study of microtremors worldwide; following this, the Nakamura method has become widely practiced. Although there are still different views on the test methods of microtremors, several studies conducted thus far have shown that microtremors contain significant information on the foundation soil layer. The application of microtremors to detect the dynamic characteristics of the soil layer and calculate the characteristics of strong ground motion is very effective [23–29]. Recently, Jiang Chang, Xuan You, and Ge Cao carried out site-effect studies on a typical rift site in the Fenwei Basin of China by using microtremor tests [23,30,31], showing that the microtremor tests were very effective in revealing the dynamic effect of the earth fissure site. However, the application of microtremors in earthquake engineering is still in the initial stages.

The microtremor signal is a stable, non-repetitive random vibration signal. The most common microtremor processing methods include the traditional Fourier methods. These methods are based on the stability and linearity of the microtremor signal. However, when

microtremor signals are collected, the inevitable interference of the surrounding environment may affect the steady state of the original signal. Therefore, this study considered the introduction of Hilbert–Huang transform (HHT), a nonlinear-based vibration signal processing method, into the processing of microtremors. Hilbert–Huang transform is a nonlinear and nonstationary vibration signal processing method first proposed by Huang in 1998 [32]. This method innovatively proposes empirical mode decomposition (EMD). Unlike the traditional signal analysis method, it does not consider any assumptions and starts from the signal to split any complex vibration signals into finite intrinsic mode function (IMF) components. Hilbert signal analysis can provide local time-frequency characteristics of the signal. Since the HHT method was proposed, it has been widely recognized in the field of signal processing and is commonly used in seismic engineering [33–36], fault identification [37,38], and aerospace [39]. As a significant breakthrough in signal analysis methods in recent years, it is still glowing with vitality.

The above studies show that there is a paucity of research on the dynamic effects of earth fissure sites. Therefore, in order to reveal the dynamic response characteristics of bedrock-buried-hill-type earth fissure sites, this paper analyzed and compared the basic characteristics of microtremor spectra of earth fissure sites through direct Fourier transform analysis and Hilbert yellow transform analysis based on microtremor testing methods, and systematically revealed the amplification effect and influence range of this type of earth fissure site, with the aim of providing a reference for their seismic design and prevention.

2. Background

2.1. Structure

The Su-Xi-Chang area is located on the southern margin of the Yangtze River Delta in China. The residual bedrock hills are scattered around Taihu Lake, and most areas are vast accumulation plains with low and flat terrain. The ground elevation is generally lower than 7 m. The geological environmental background of the Su-Xi-Chang area has determined the distribution and development characteristics of earth fissures in this area. The geomorphic pattern of the base in this area was caused by the Yanshan Movement that occurred at the end of the Mesozoic era. The Yanshan Movement alternates frequently, and the level of erosion is low. Hence, due to intense tectonic activity, the ancient terrain experiences successive rises. Quaternary strata are widely distributed in this area, with thicknesses of 150–260 m, generally increasing from southwest to northeast (Figure 1). The inherited differential subsidence movement of the base structure has always played a controlling role in the quaternary sedimentation in this area. This geological structure has retained abundant groundwater since ancient times [3]. It is a typical geological formation in which the second confined aquifer buried is widely distributed and has a high water yield, which led to the large-scale development and utilization of groundwater resources in 1970. The long-term overexploitation of groundwater and the sharp decline in the water level resulted in severe land subsidence in the Su-Xi-Chang area, and an earth fissure was subsequently formed [6].

Typical bedrock-buried-hill earth fissures developed in the Su-Xi-Chang area were surveyed and investigated in this paper. Six typical earth fissures were ultimately identified as the study object: the F1 and F2 earth fissures in Yingguoan Village, Wuxi City; the F3 and F4 earth fissures in Guangming Village, Wuxi City; the F6 earth fissure in Chaqiao, Wuxi City; and the F9 earth fissure in Hetang, Jiangyin City.

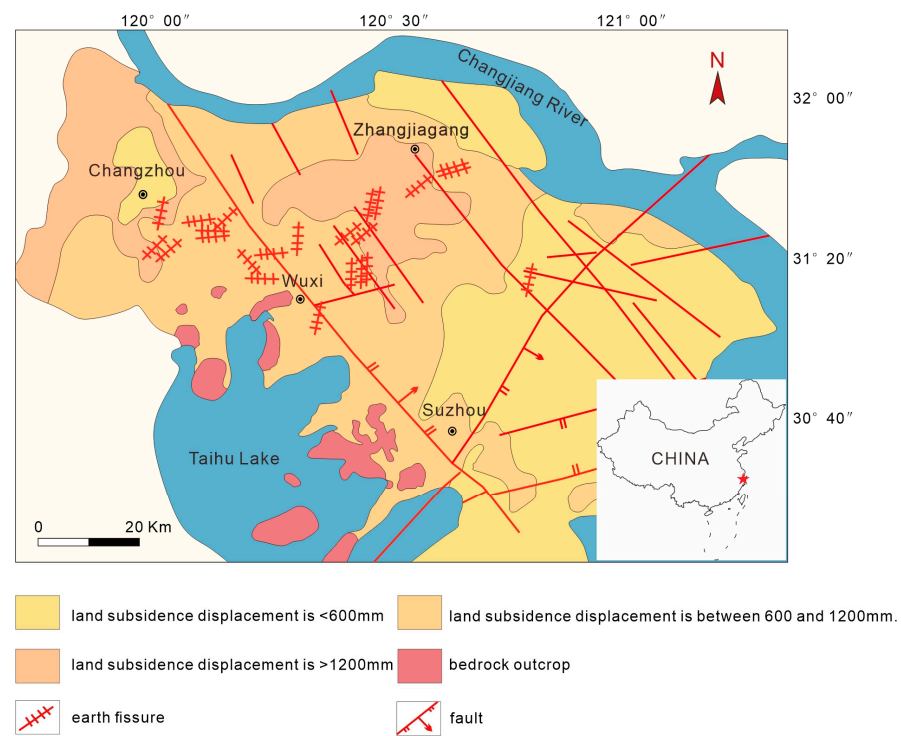


Figure 1. Geographical location and structure map of the Su-Xi-Chang area.

2.2. Earth Fissures

2.2.1. Earth Fissures in Yingguoan (F1–2, 1991)

The F1 and F2 earth fissures are located in Yingguoan Village, Shitangwan Town, Wuxi (Figure 2), and began in 1991. At present, there are two nearly parallel earth fissure belts with lengths of approximately 2000 m in the NE direction. F2 has experienced greater differential settlement than F1. The mountain terrain significantly differs from north to south, and the site is located above ancient, submerged hills that trend in a NE–NEE direction. In addition, the ancient buried ridge is shallow at the uplifted section of the hill, and the thickness is less than 40 m, whereas the buried depth and consistency are significantly greater on the north and south sides. The thickness varies significantly across the entire site. In addition, the differential settlement of soil after groundwater mining has eventually induced earth fissures. Figure 2 depicts the 120 m long survey line that runs through F1 and F2.

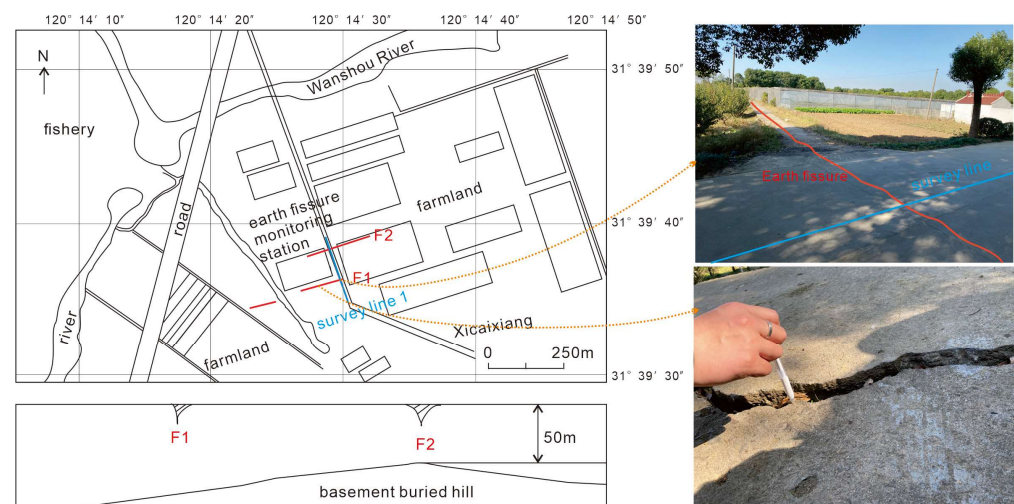


Figure 2. Distribution map and profile of F1–2.

2.2.2. Earth Fissures in Guangming Village (F3–4, 1998)

Guangming Village is home to F3 and F4, in Xibei Town, Wuxi City, near Hetang Town, Jiangyin City. F3 is a differential ground-subsidence type of earth fissure dominated by pumping. Earth fissures began to appear in Guangming Village in 1998 and were first discovered in a resident's home in Yangshuli. The earth fissures rapidly developed, propagating in village groups such as Tangjiali, Shuiqu Lane, Xujiashuji, and Jijiaba in Guangming Village. Thus far, the earth fissures in Guangming Village have caused serious damage to the area. Wherever an earth fissure appears, residential houses are damaged, door frames are deformed, entire houses become tilted, and the earth becomes significantly staggered (Figure 3c), resulting in more than 400 unsafe houses. The earth fissures in Guangming Village are generally NE fissures and appear in clusters. The primary and secondary cracks are roughly parallel. The surface traces are mainly concentrated in residential homes and are most evident at the entrance of Yangshuli, with a surface dislocation of approximately 20 cm (Figure 3b). According to the survey, the underlying bedrock surface is uneven, the loose layer at the uplift is only 60 m, and the earth fissures in this area are closely related to groundwater exploitation. When the first earth fissure appeared in Guangming Village, it was during a period of rapid decline in groundwater (Figure 4) [4]. Under the mutual impact of various factors, the formation of earth fissures was induced; since then, the groundwater level has gradually decreased, and fissures have begun to develop continuously. The entrance of Yangshuli, where the situation is the most serious, is at the top of the buried bedrock hill. The survey line is arranged at the village entrance, where the F3 main crack is exposed in front of a residential building (Figure 3).

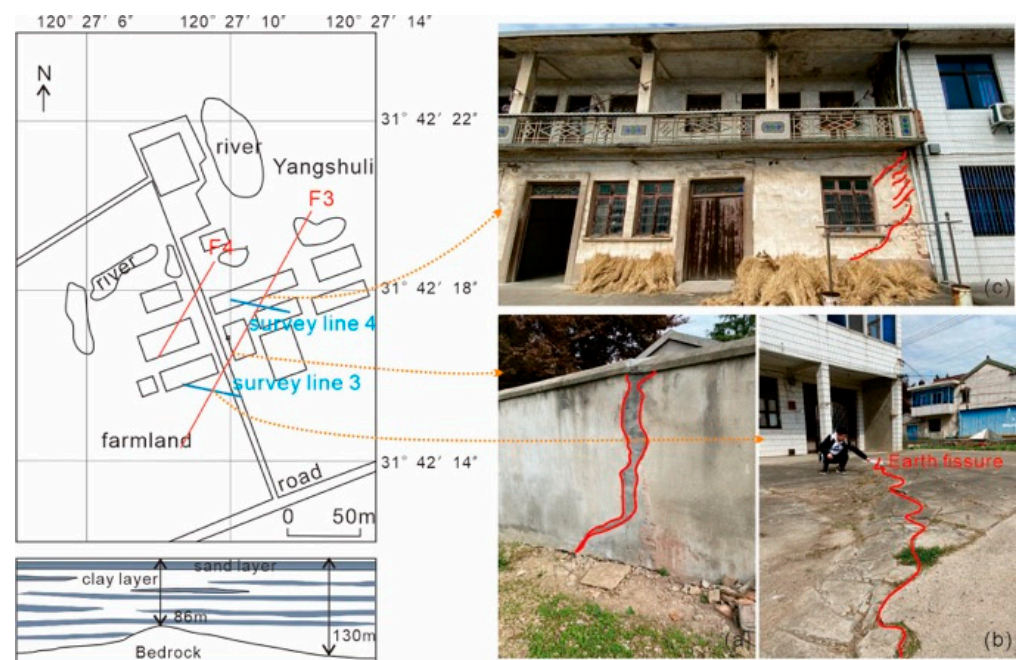


Figure 3. Distribution and earth fissure situation in Guangming Village (F3 and F4): (a–c) F3 earth fissure disaster.

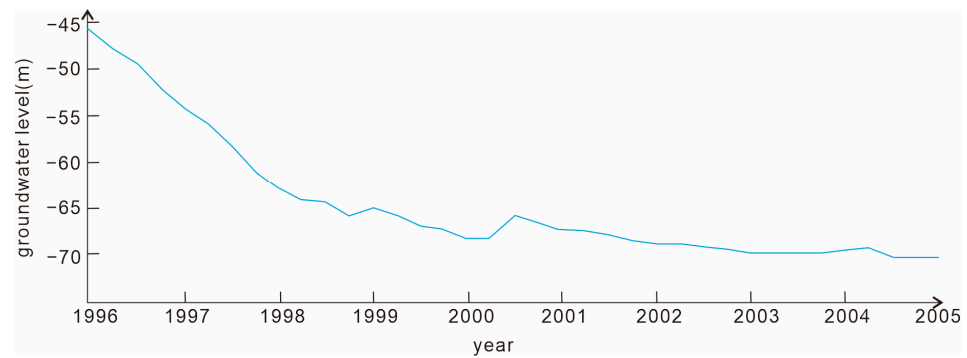


Figure 4. Changes in the groundwater level near Guangming Village from 1996 to 2005.

2.2.3. Earth Fissures in Chaqiao (F6, 1992)

The Chaqiao earth fissure is the most extensive in Xishan City. It began in 1992, starting from Longdangtou (F5) in Shanhe Village and subsequently extending to Jijianong in Houshan Village, Denggengxiang (F6) in Shanhe Village, Chuanqiaotou, and other areas. The scale of damage in each village varies, but the earth fissures are distributed in a north–south direction (Figure 5). F6 is located in Denggengxiang, with an evident surface trace; the earth fissure is approximately 80 m long and 30 m wide.



Figure 5. Distribution and earth fissure situation in Chaqiao (F6): (a,b) F6 earth fissure disaster.

2.2.4. Earth Fissures in Hetang, Jiangyin City (F9, 1995)

The two most representative earth fissures in Jiangyin are located in Changjing (F8) and Hetang (F9) Towns in the south. The F8–9 earth fissures have been developing since 1995. The direction of the two main cracks is the same, and the main fracture zone is distributed in the NE direction where the earth fissure situation is the most serious. F8 once crossed a nine-story building of the local Shuangping group and destroyed it [6]. Subsequent investigation found that the old site had been completely demolished, but the earth fissure was still active. At that time, the water conservancy and agricultural technology station had been transformed into the Huanghong textile factory, and several earth fissures were found in the textile factory, resulting in serious damage to its walls (Figure 6); F9 had mainly developed in the building complex on the north side of the Hetang community. The main fracture trend is NE 20°, and the width is approximately

20–60 m. The fracture zone is composed of one main fracture and three to four secondary fractures, extending up to approximately 500 m. It is generally found in a differential settlement mode, high in the east and low in the west. According to the investigation, the buried bedrock ridge at the development of the earth fracture is consistent with the earth fissure, and the shallowest buried depth of the ridge is approximately 64 m. The thickness of loose overburden on both sides of the mountain is generally 140–150 m (Figure 7). The area of unsafe buildings caused by F9 could be as high as 8763.8 m² [40]. At present, a few unsafe buildings are still preserved. Earth fissure damage has been found in an old tax bureau and the residential area in the north (Figure 8), and the survey line is located in the residential area in the north (Figure 7).



Figure 6. Earth fissure situation at the Jiangyin Huanghong textile factory (F8).

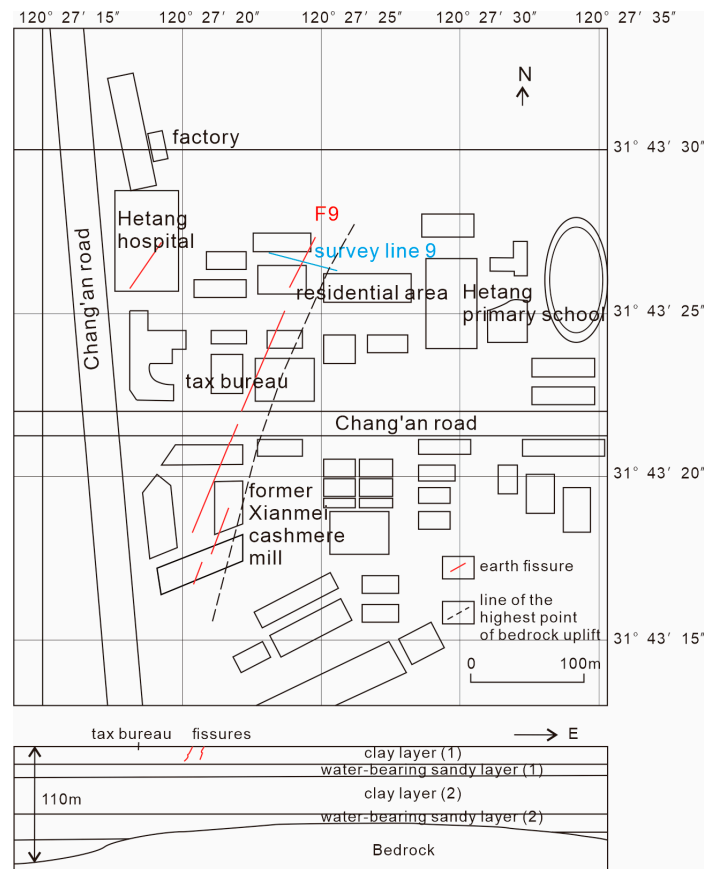


Figure 7. Distribution map and profile of F9.

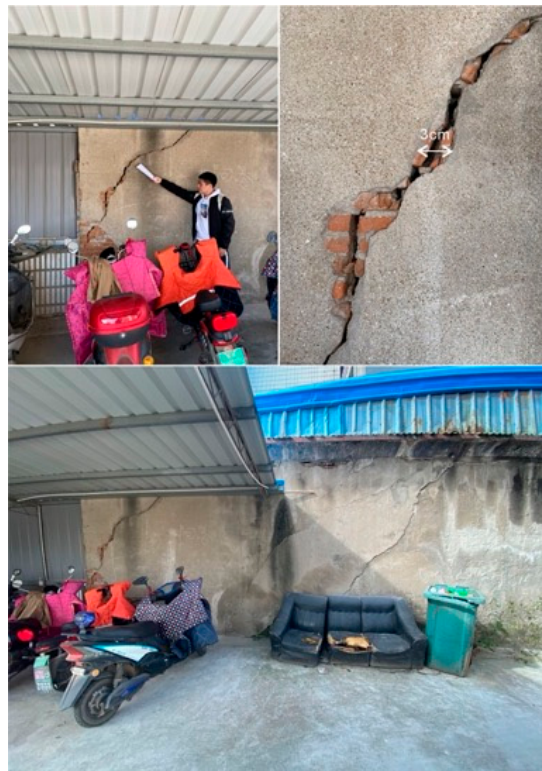


Figure 8. Wall of a tax bureau that has cracked under the influence of fissures (F9).

3. Methodology

3.1. Microtremor Test

Microtremors are microseismic signals that vibrate continuously on the Earth's surface. The spectral characteristics of microtremor signals can reflect the dynamic properties of the site. Since the local site conditions, seismic source characteristics, and testing instruments remain unchanged during the testing process, the effect of earth fissures on the site's dynamic response can be revealed based on the changing pattern of microtremor spectral features across different locations at the site.

The servo velocity network seismometer (CV-374AV) manufactured by Japan's Tokyo Vibration Measurement Company (Tokyo, Japan) features high sensitivity, portability as well as a long measurement time, and can be used to effectively monitor microtremor data. The test instrument sampling frequency had a range of 0.1–100 Hz, and could simultaneously monitor the data in three orthogonal directions.

The selection of survey lines was as previously mentioned. In principle, each survey line had 18 survey points and a total length of 60 m. The survey points were arranged densely near the earth fissure, and the hanging and heading sides were arranged symmetrically (Figure 9). The microtremor data were collected at night.

Each measuring point collected a section of microtremor data of 600 s, intercepted the relatively stable wave band, and considered the data for 10 s as a group for analysis.

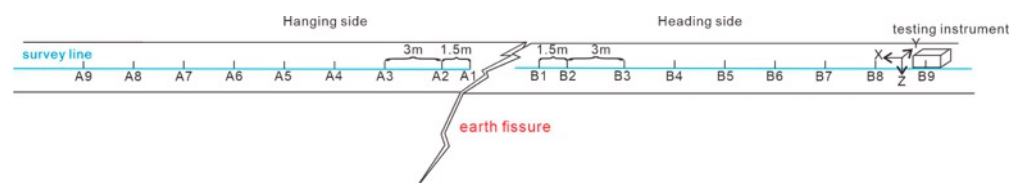


Figure 9. Schematic diagram of the survey line layout.

3.2. Data Processing Method

Fourier transform is the conversion of a continuous signal that is nonperiodic in the time domain into a continuous signal that is nonperiodic in the frequency domain. A certain number of trigonometric functions are used to arbitrarily characterize nonperiodic complex functions. However, because Fourier transform uses a global definition of the signal, there are some crucial restrictions in Fourier spectral analysis: (1) the system must be linear, and (2) the data must be strictly periodic or stationary. Therefore, the nonlinear data analysis method should be considered when the data collected do not satisfy these strict requirements. Therefore, we introduced the Hilbert–Huang transform method, which involves an EMD method that can decompose any complex dataset into a finite and often small number of IMFs that allow for well-behaved Hilbert transforms. The decomposition is based on the local characteristic time scale of the data applicable to nonlinear and nonstationary processes. The final presentation of the results is an energy–frequency–time distribution, designated as the Hilbert spectrum. By integrating the Hilbert spectrum with time, we can obtain the marginal spectrum, which offers a measure of the total amplitude (or energy) contribution from each frequency value [30].

Figure 10 shows the EMD decomposition process of the 10 s microtremor data. The signal was efficiently decomposed into seven IMF components and a residual term. The frequency of the decomposed IMF components decreased in turn, and there was no sinusoidal function of the decomposed IMF components. The HHT method provides the first innovative improvement in the basic signal and frequency definitions, considering that the basic components that make up a signal are no longer sinusoidal, but rather consist of a finite number of intrinsic modal functions. The EMD decomposition process has been applied in related seismic engineering fields such as the dynamic response of slopes under seismic activity [41], the decomposition of seismic signals [42], and the seismic response of soft soils [43], showing the effectiveness of the EMD sieving method of Hilbert–Huang transform for processing complex nonlinear signals.

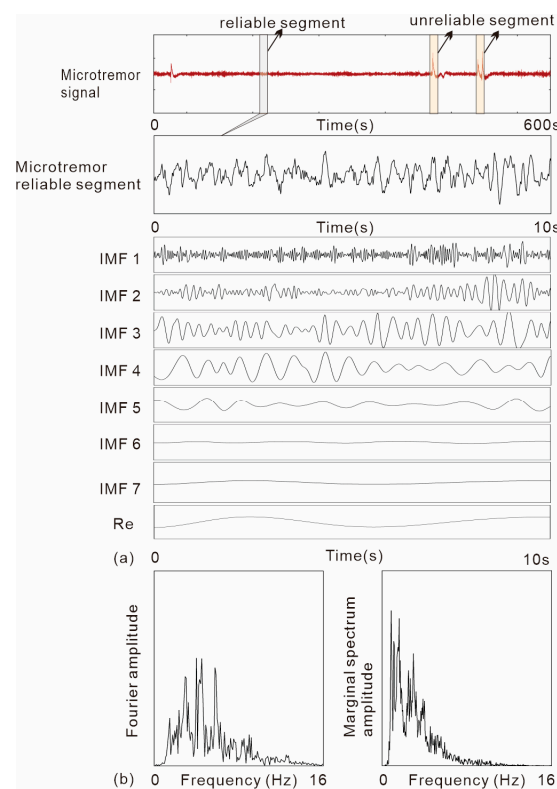


Figure 10. Data processing: (a) resulting empirical mode decomposition components from the microtremor signal; (b) Fourier and marginal spectra.

In order to investigate the dynamic response characteristics of the earth fissure site, based on fast Fourier transform and Hilbert–Huang transform, the effect of the existence of an earth fissure on the basic characteristics of the dynamic response within the site can be revealed by comparing the Fourier spectrum and the marginal spectrum of each spectral feature of the 18 measurement points on both sides of the earth fissure. A comparison of the two methods of spectral analysis of microtremors not only revealed the dynamical characteristics of earth fissure sites more accurately, but also opens up a completely new way of thinking for the future acquisition of spectral characteristics reflected by microtremors.

4. Results

4.1. Spectral Analysis

The results of the microtremor spectral analyses of different sites showed that the Fourier and marginal spectral characteristics were basically consistent for sites with close soil conditions. Earth fissures did not change the predominant frequency of the sites and all the different earth fissures had significant amplification effects on the dynamic response characteristics of the sites.

Based on the aforementioned Fourier and HHT analysis of the microtremor data collected from the five survey lines, the results of each site are shown in (a) and (b), respectively, in Figures 11–16. The same method yielded consistent spectral patterns in the hanging and heading sides of the earth fissure sites; a comparison of the analytical results of those two methods showed that similar to the results of the previous analysis of the 10 s microtremor signal, the Fourier spectral patterns were always comprehensive, and roughly concentrated within 0–15 Hz. In contrast to the marginal spectral energy distributed between 0 and 10 Hz, the Fourier spectral energy distribution range was extensive and the spectral pattern was relatively broad. The superior amplitude of the marginal spectrum was always more significant than that of the Fourier spectrum. The position of the marginal spectrum amplitude was in front, comparatively; that is, the predominant frequency with HHT was lower and more concentrated than that with Fourier transform. Based on the spectral patterns reflected by different survey lines, the marginal spectrum of the same fissure site was similar in shape to the Fourier spectrum. However, the marginal spectrum resembled a lateral narrowing of the Fourier spectrum, narrowing it to a lower frequency interval.

To visualize the relationship between the amplitude of each point on the survey line and the distance of the earth fissure, we directly analyzed the graphs in Figures 12c, 13c, 14c, 15c and 16c, where the points represent the average amplitude in the three directions of the measurement point. The results of both analysis methods showed that there was a significant amplification effect of the bedrock-buried-hill-type earth fissure on the response of the sites, as indicated by a significant increase in the amplitude of the measured points closest to the fissures, and the amplitude of the site gradually decreased with an increasing distance from the earth fissure. This then gradually tapered off in areas farther from the earth fissure. Figure 12c further confirms this amplification phenomenon, where F2 and F1 are the primary and secondary fissures of the bedrock-buried-hill structural site on the Yingguoan, respectively. The amplitude of the entire site reached its peak in the hanging side of the central fissure F2 and then gradually attenuated. In an area far from F2, the curve tended to be stable, but was then affected by the secondary fissure F1; the curve inversion showed an increasing trend. Compared to the two broken red and black lines in the figure, the amplitude of the HHT method was always greater than that of the Fourier method, and the difference between these two values at the earth fissure was more significant. Subsequently, the difference slowly decreased further from the fissures, and the two lines were nearly parallel.

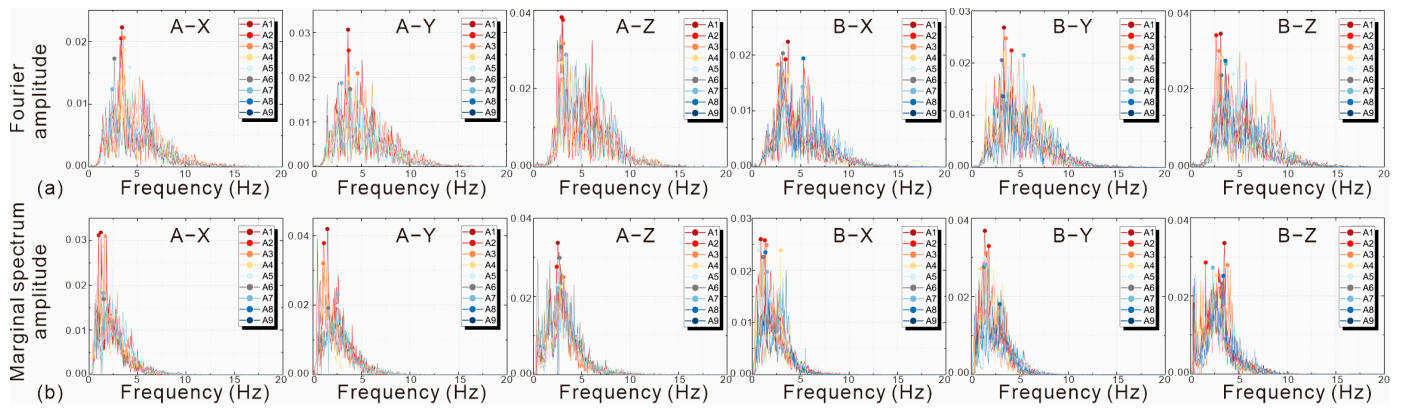


Figure 11. F1 spectra results: (a) Fourier spectrum; (b) marginal spectrum.

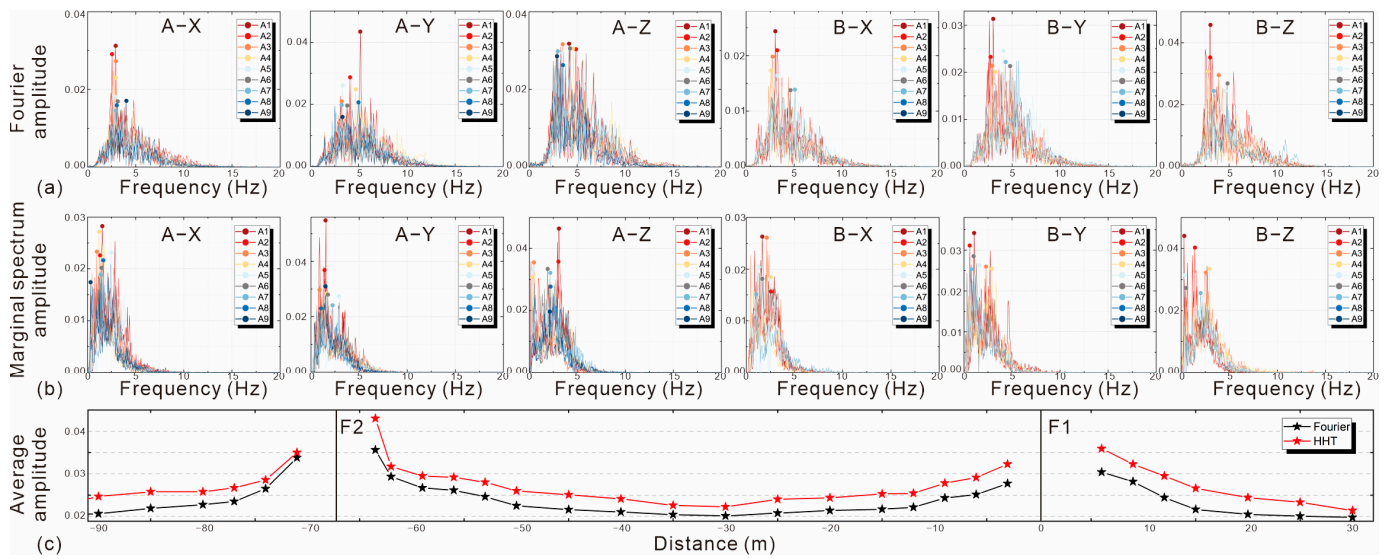


Figure 12. F2 spectra results: (a) Fourier spectrum; (b) marginal spectrum; (c) average amplitude curve.

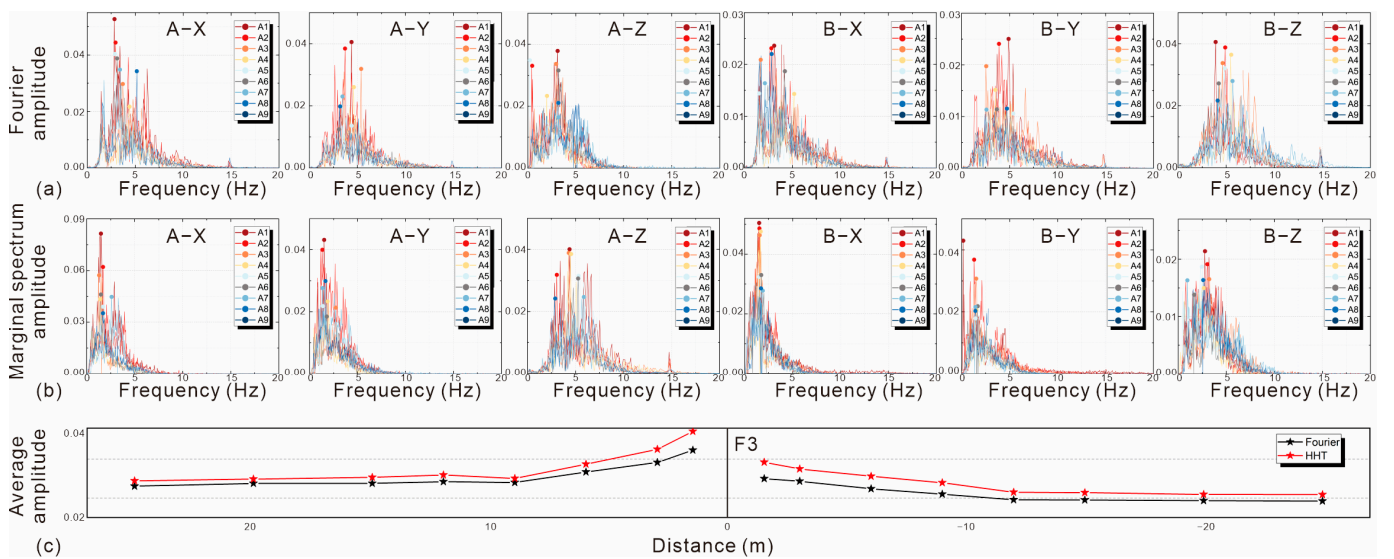


Figure 13. F3 spectra results: (a) Fourier spectrum; (b) marginal spectrum; (c) average amplitude curve.

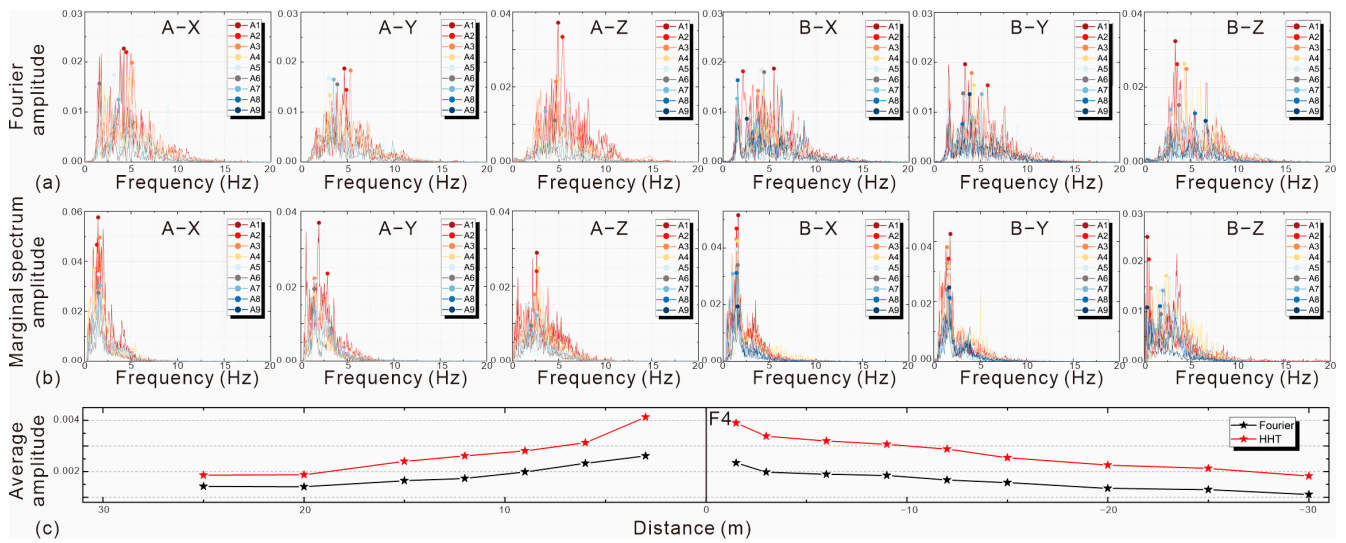


Figure 14. F4 spectra results: (a) Fourier spectrum; (b) marginal spectrum; (c) average amplitude curve.

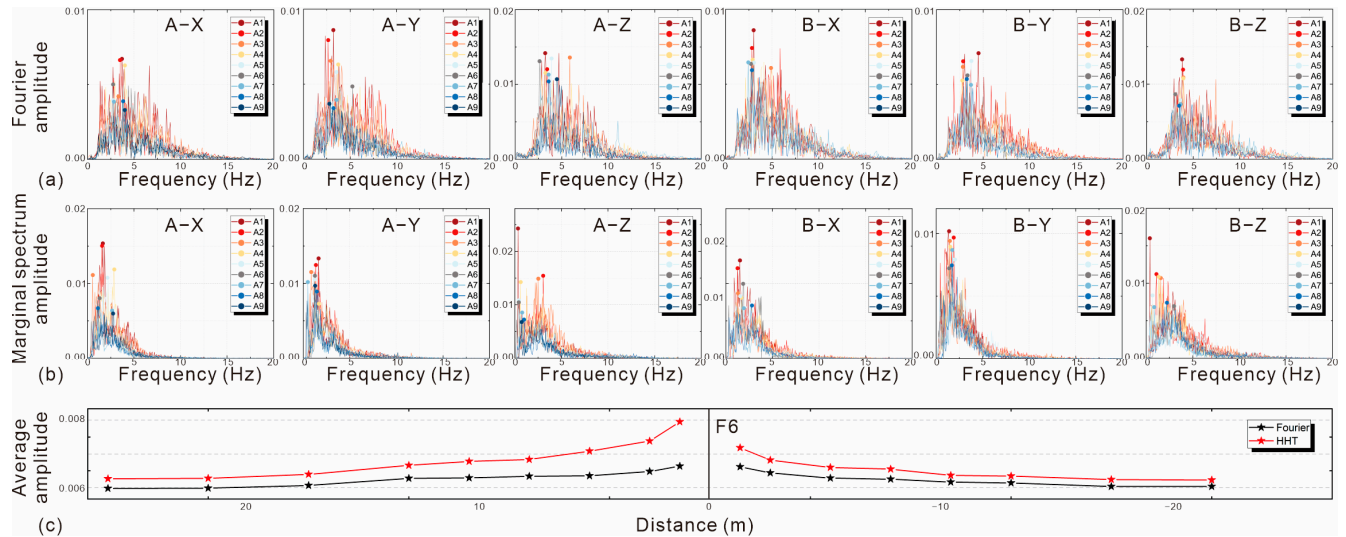


Figure 15. F6 spectra results: (a) Fourier spectrum; (b) marginal spectrum; (c) average amplitude curve.

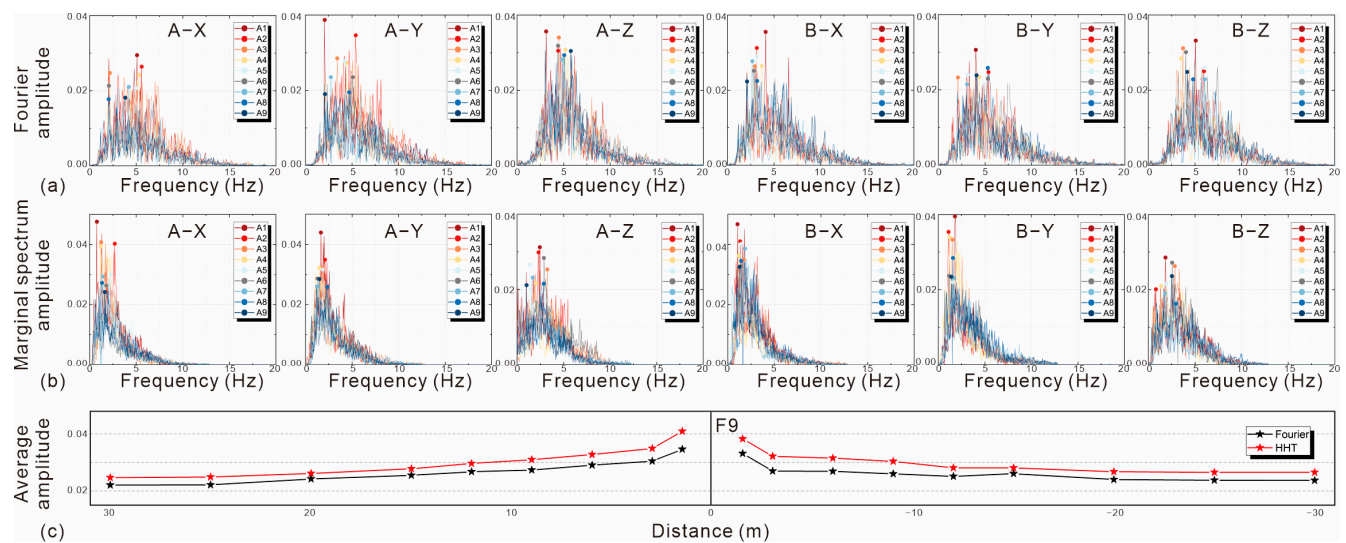


Figure 16. F9 spectra results: (a) Fourier spectrum; (b) marginal spectrum; (c) average amplitude curve.

4.2. Amplification Factor Analysis

From the analyses of the five microtremor survey lines, the average peak values of the spectra at each site tended to be stable at the measurement points within 25–30 m from the earth fissures, and the peak values were kept within a certain low threshold, which can be regarded as the smooth amplitude of the original site not being affected by the amplification effect of the fissures. However, since the overall amplitude varied from site to site, we needed to assess the characterization of the amplification effect at these earth fissure sites on an identical amplitude scale.

The ratio of the average peak spectrum of each measurement point to the original site's peak smooth spectrum is the magnitude of the amplification of the site by earth fissures, defined as the "amplification factor":

$$AF(i) = Ai/\omega \quad (1)$$

$$BF(i) = Bi/\omega \quad (2)$$

where $i = 1, 2, 3, \dots, 9$; $AF(i)$ is the amplification factor of each measurement point on the hanging side; and $BF(i)$ is the amplification factor of each measurement point on the heading side.

Figure 17 shows a broken line diagram of the amplification factors for the Fourier and HHT methods at each site.

The amplification degree of the dynamic response of the bedrock-buried-hill-type earth fissure at the site can be seen in Figure 17. The decay pattern of the amplification factor is consistent with the average amplitude fold, as described earlier. Based on the horizontal comparison of Figure 17, it was found that the extreme values of the Fourier method ranged from 1.8 to 1.5 for the hanging side amplification factor and 2.1 to 1.3 for that of the heading side; the extreme values of the HHT method ranged from 2.3 to 1.6 for the hanging side amplification factor and 2.1 to 1.4 for that of the heading side. It can be seen that there was a slight difference in the dynamic amplification response between the two sides of the bedrock-buried-hill-type fissure site, that structures in the area of the two sides closest to the earth fissure may be exposed to seismic intensities well in excess of the original level of containment, by more than double, and the fortification intensity of the hanging sides needs to be considered to be slightly higher than that of the heading.

The amplification factor of the hanging side was more significant than that of the heading side for the same fissure site, and this can be attributed to the concentration of bedrock-buried-hill-type earth fissures at the top of the mountain; symmetrical cracks can be found on both sides, similar to the Chinese character 'eight'. The fissures on either side were always in the descending state of the hanging side, which is a standard normal fault. Therefore, the hanging side is more active, and the dynamic amplification effect in the hanging side of the earth fissure site is more significant. In a longitudinal comparison of Figure 17, the extreme value of the amplification factor obtained by the Fourier method was always lower than that of the HHT method for the same fissure site. The amplification factor of the HHT method was on average higher than that of the Fourier method by approximately 0.1–0.2, with the maximum difference reaching 0.7 (Site 6, hanging side). In the far field, approximately 15–30 m away from the fissure, the difference between the amplification factors obtained by the two methods gradually decreased until they converged.

When the amplification factor converges to 1, the dynamic response of the site can be considered to be unaffected by earth fissures. Therefore, we can divide a safe avoidance distance for building construction, and the buildings in this area can maintain the original seismic fortification level. From the HHT and Fourier amplification factors, it can be concluded that the safety distances were relatively close. However, the range of influence slightly varied depending on the site, with the amplification factors generally stabilizing at approximately 25 m.

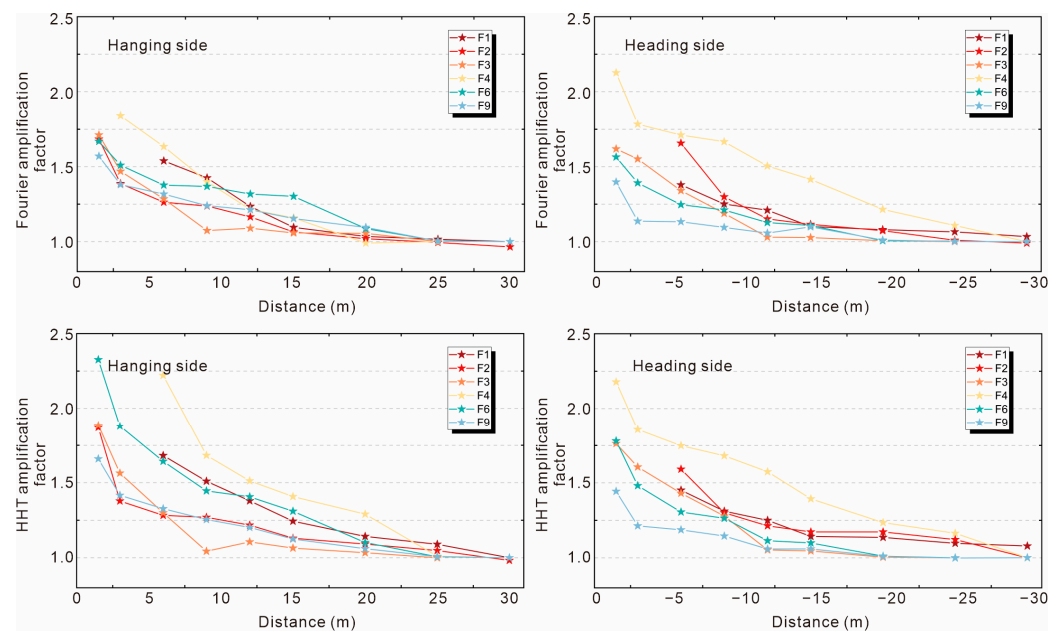


Figure 17. Magnification factor line chart.

The analyses show that both the Fourier and HHT methods are valid for the dynamic response of earth fissure sites, as revealed by the microtremor data. The two analyses yielded the same maximum range of dynamic amplification for bedrock-buried-hill-type earth fissure sites, with both sides at about 25 m. The surface structures beyond this distance could maintain the seismic fortification level of the original area. The extreme value of the amplification factor of the bedrock-buried-hill-type fissure site obtained by the two analysis methods was close, but the Fourier method was slightly lower than the HHT method. The extreme value of the amplification factor of the hanging side was about 1.8–2.3, while the extreme value of the amplification factor of the heading was about 2.1. In practice, the basic design of the seismic acceleration of the structure close to a bedrock-buried-hill fissure should be adjusted to more than twice the original value.

5. Discussion

Hilbert–Huang transform is based on a nonlinear, nonsmooth signal analysis method compared with the traditional Fourier spectral analysis method, without strict assumptions. The results of this study prove the effectiveness of the HHT method in the processing of microtremor data using nonlinear analysis. However, there are still many areas in which the HHT method can be applied. Many ‘nonstationary’ segments that are evidently disturbed can be seen by the naked eye from the microtremor data collected. Generally, we try to avoid selecting such microtremor data for processing. We can use the HHT method to screen such evident interference segments with EMD, remove individual IMF components, and restore signals (such as regular factory machine and passing car vibrations), thus achieving a ‘filtering’ process that allows the affected microtremor data to be restored to their original state, significantly improving the efficiency of microtremor processing, which is worthy of further research.

Moreover, the difference between the Fourier and HHT methods in the near- and far-field results of earth fissures has attracted our attention. We should investigate whether the reason for the above phenomenon is the interval tending to an unstable state being larger in the far-field area after being affected, or the high overall amplitude of microtremors near the fissures, due to which the Fourier method supplements simpler harmonics, resulting in the most significant difference between the two methods on both sides closest to the fissure. From the point of view of seismic safety, the amplification factors given by each of the two analyses should be considered together. The HHT method can more accurately reflect

the real frequency component of the signal in the case of interference by decomposing the signal from the vibration mode of the signal itself. This provides a new scope for analysis in future applications of microtremor testing.

This study focused on a unique bedrock-buried-hill-type earth fissure site in China, filling the research gap on the dynamics of this type of fissure site. The results confirm that bedrock-buried-hill fissures in the Su-Xi-Chang area have a significant amplification effect on the dynamic response of the site, which should attract the attention of scholars to this topic. This study also clarifies the dynamic response law and its influence range on bedrock-buried-hill earth fissure sites and provides a reference for seismic fortification planning in the Su-Xi-Chang area as well as a basis for the seismic design of future engineering structures and the disaster prevention and mitigation of related sites. In future research, if different engineering structures are constructed at this type of earth fissure site, more systematic and comprehensive guidance on seismic fortification can be provided from the perspective of the vibration response characteristics.

6. Conclusions

The aim of this study was to obtain the dynamic response characteristics of bedrockburied-hill-type earth fissure sites based on six typical earth fissure sites in the Su-Xi-Chang area, China. Through a systematic microtremor test, Fourier spectrum analysis, and Hilbert–Huang transform analysis, the variation law of the dynamic amplification effect of bedrock-buried-hill-type earth fissure sites was compared and revealed.

Bedrock-buried-hill earth fissures have a significant amplification effect on the dynamic response of the site, which indicates that the spectral peaks of measuring points close to the earth fissure are significantly higher than those far away from the fissure. This shows that the strength of the dynamic response of the buildings around the bedrock-buried-hill-type earth fissure under seismic conditions is expected to be much higher than the original field dynamic response under the condition of no fissure sites.

Based on the fact that the peak value of the spectrum at each measuring point on the site tended to be stable after 25–30 m from the earth fissure, the amplification factors of the direct Fourier spectrum and Hilbert–Huang marginal spectrum were calculated for the stationary reference index of the site amplification effect, and the basic characteristics of the amplification effect of the bedrock-buried-hill-type fissure site were revealed on the same order of magnitude.

Fourier and Hilbert–Huang transform amplification factors showed that the dynamic amplification effect of bedrock-buried-hill-type fissure sites followed the same change pattern; that is, the amplification factor closest to the earth fissure was the highest, and it gradually decreased with the distance from the earth fissure.

The furthest influence range of the dynamic amplification effect of bedrock-buried-hill-type fissure sites was about 25 m. From the perspective of seismic fortification, buildings in areas 25 m away from the earth fissure can maintain their original seismic fortification level.

The extreme value of the amplification factor for bedrock-buried-hill earth fissure sites was around 2.0, indicating that the buildings at the site closest to the earth fissure should be considered in order to adjust the basic design seismic acceleration to about two times the original one, and that the hanging side should be higher than that of the heading side as much as possible.

Both Fourier and HHT methods are effective in processing microtremor data to reveal the site's dynamic response characteristics, but the Fourier analysis method may underestimate the amplification extremes of earth fissure sites. In the future, the two spectral analysis methods should be considered comprehensively to reflect the dynamic response characteristics of the site as accurately as possible and to provide references for the actual seismic fortification work.

Author Contributions: Conceptualization, supervision, and methodology, Y.D.; Investigation, G.C., J.C., Y.X. and D.N.; Software, formal analysis and writing—original draft preparation, G.C.;

Writing—review and editing, Y.D. and G.C.; Project administration, H.M.; Funding acquisition, Y.D. and H.M. All authors have read and agreed to the published version of the manuscript.

Funding: This research was supported by the National Natural Science Foundation of China (Grant No. 41772275), Yahong Deng; the Fundamental Research Funds for the Central Universities (No. 300102268203), Yahong Deng; the Natural Science Basic Research Program of Shaanxi Province (2022JQ-289), Yahong Deng; the Fundamental Research Funds for the Central Universities, CHD (300102262505), Huandong Mu; and the Key Research and Development Projects of Shaanxi Province (No. 2022SF-197), Huandong Mu.

Institutional Review Board Statement: Not applicable.

Informed Consent Statement: Not applicable.

Data Availability Statement: The raw data supporting the conclusions of this article will be made available by the authors on request.

Conflicts of Interest: The authors declare no conflicts of interest.

References

- Peng, J.; Qiao, J.; Sun, X.; Lu, Q.; Zheng, J.; Meng, Z.; Xu, J.; Wang, F.; Zhao, J. Distribution and generative mechanisms of ground fissures in China. *J. Asian Earth Sci.* **2020**, *191*, 104218. [[CrossRef](#)]
- Peng, J.; Sun, X.; Lu, Q.; Meng, L.; He, H.; Qiao, J.; Wang, F. Characteristics and mechanisms for origin of earth fissures in Fenwei basin, China. *Eng. Geol.* **2020**, *266*, 105445. [[CrossRef](#)]
- Wang, G.Y.; You, G.; Shi, B.; Qiu, Z.L.; Li, H.Y.; Tuck, M. Earth fissures in Jiangsu province, China and geological investigation of Hetang earth fissure. *Environ. Earth Sci.* **2010**, *60*, 35–43. [[CrossRef](#)]
- Gao, Z.; Zhu, Q.; Ji, Y.; Chen, X. The research on the distribution feature, genetic type and countermeasure about ground fissure events in Jiangsu province of China. *J. Seism.* **1997**, *1*, 1–10.
- Zhu, J.Q.; Zhu, X.X. Genetical analysis and countermeasures of ground fracture disasters in Hetang town, Jiangyin city. *Hydrogeol. Eng. Geol.* **1998**, *25*, 14–15.
- Wang, G.Y.; Shi, B.; Wang, X.M. Land subsidence and earth fissures in southern Jiangyin. *Hydrogeol. Eng. Geol.* **2009**, *36*, 117–122. [[CrossRef](#)]
- Wu, J.C.; Zhou, G.J.; Wu, Y.L. Research on earth fissures in Guangming village of Wuxi city. *J. Geol.* **2013**, *37*, 203–207. [[CrossRef](#)]
- Chen, G.M.; Wang, X.M.; He, H.S.; Xu, X.L.; Wu, J.H. Formation mechanism analysis on ground fissure based on 3D seismic exploration data in Yinguo'an area, Wuxi city. *Hydrogeol. Eng. Geol.* **2006**, *33*, 117–119+123. [[CrossRef](#)]
- Wu, J.C.; Ye, S.J.; Wu, J.F.; Wang, G.Y.; Zhang, Y. Research on nonlinear coupled modeling of land subsidence in Suzhou, Wuxi and Changzhou areas, China. *Hydrogeol. Eng. Geol.* **2007**, *34*, 11–16. [[CrossRef](#)]
- Spadi, M.; Tallini, M.; Albano, M.; Cosentino, D.; Nocentini, M.; Saroli, M. New insights on bedrock morphology and local seismic amplification of the Castelnuovo village (L'Aquila Basin, Central Italy). *Eng. Geol.* **2022**, *297*, 106506. [[CrossRef](#)]
- Mooney, W.D.; Ginzburg, A. Seismic measurements of the internal properties of fault zones. *Pure Appl. Geophys.* **1986**, *124*, 141–157. [[CrossRef](#)]
- Liu, N.; Huang, Q.; Ma, Y.; Bulut, R.; Peng, J.; Fan, W.; Men, Y. Experimental study of a segmented metro tunnel in a ground fissure area. *Soil Dyn. Earthq. Eng.* **2017**, *100*, 410–416. [[CrossRef](#)]
- Liu, N.; Huang, Q.; Wang, L.; Fan, W.; Jiang, Z.; Peng, J. Dynamic characteristics research of a ground fissure site at Xi'an, China. *Tunn. Undergr. Space Technol.* **2018**, *82*, 182–190. [[CrossRef](#)]
- Liu, N.; Feng, X.; Huang, Q.; Fan, W.; Peng, J.; Lu, Q.; Liu, W. Dynamic characteristics of a ground fissure site. *Eng. Geol.* **2018**, *248*, 220–229. [[CrossRef](#)]
- Xiong, Z.; Wang, Y.; Chen, X.; Xiong, W. Seismic behavior of underground station and surface building interaction system in earth fissure environment. *Tunn. Undergr. Space Technol.* **2021**, *110*, 103778. [[CrossRef](#)]
- Omori, F. On micro-tremors. *Bull. Imp. Earthq. Investig. Comm.* **1908**, *2*, 1–6.
- Kanai, K. Measurement of microtremor I. *Bull. Earthq. Res. Inst.* **1954**, *32*, 199–209.
- Aki, K. Space and time spectra of stationary stochastic waves, with special reference to microtremors. *Bull. Earthq. Res. Inst.* **1957**, *35*, 415–456. [[CrossRef](#)]
- Kagami, H.; Duke, C.M.; Liang, G.C.; Ohta, Y. Observation of 1- to 5-second microtremors and their application to earthquake engineering. Part II. Evaluation of site effect upon seismic wave amplification due to extremely deep soil deposits. *Bull. Seism. Soc. Am.* **1982**, *72*, 987–998. [[CrossRef](#)]
- Kagami, H.; Okada, S.; Shiono, K.; Oner, M.; Dravinski, M.; Mal, A.K. Observation of 1-to 5-second microtremors and their application to earthquake engineering. Part III. A two-dimensional study of site effects in the San Fernando valley. *Bull. Seismol. Soc. Am.* **1986**, *76*, 1801–1812. [[CrossRef](#)]

21. Ohta, Y.; Kagami, H.; Goto, N.; Kudo, K. Observation of 1-to 5-second microtremors and their application to earthquake engineering. Part I: Comparison with long-period accelerations at the Tokachi-Oki earthquake of 1968. *Bull. Seismol. Soc. Am.* **1978**, *68*, 767–779. [[CrossRef](#)]
22. Nakamura, Y. A method for dynamic characteristics estimation of subsurface using microtremor on the ground surface. *Q. Rep. RTRI.* **1989**, *30*, 25–33. Available online: <http://worldcat.org/oclc/3127232> (accessed on 1 January 1989).
23. Chang, J.; Deng, Y.; Xuan, Y.; Yan, Z.; Wu, W.; He, J. The dynamic response of sites with earth fissures as revealed by microtremor analysis—A case study in the Linfen Basin, China. *Soil Dyn. Earthq. Eng.* **2020**, *132*, 106076. [[CrossRef](#)]
24. Guo, M.Z.; Ren, F.H. The microtremor methods for dynamics measurement of sites. *World Inf. Earthq. Eng.* **2005**, *21*, 139–142. [[CrossRef](#)]
25. Hu, Z.Y.; Yang, S.S.; Li, H. Ground microtremor test and its application in evaluation of sites. *World Earthq. Eng.* **2011**, *27*, 211–218.
26. Shi, L.J.; Chen, S.Y. The applicability of site characteristic parameters measurement based on micro-tremor's H/V spectra. *J. Vib. Shock* **2020**, *39*, 138–145. [[CrossRef](#)]
27. Tao, X.X.; Liu, C.W.; Guo, M.Z. A review of microtremor study in engineering site rating. *Earthq. Eng. Eng. Vib.* **2001**, *21*, 18–23.
28. Yan, W.J.; Wu, Z.J.; Che, A.L.; Zhong, P.F.; Chen, Y.J. Microtremor measurement research of amplification effect in the loess site of the Minxian-Zhangxian MS6.6 earthquake. *China Earthq. Eng. J.* **2013**, *35*, 477–482. [[CrossRef](#)]
29. Zhang, L.G.; Deng, Y.H.; Xue, J.; Wang, H.; Liu, Q.; Yang, Y. Preliminary research on dynamic response characteristics of microtremor at ground fissure sites—illustrated with F6 ground fissure in Xi'an. *J. Eng. Geol.* **2017**, *25*, 784–793. [[CrossRef](#)]
30. You, X.; Yahong, D.; Jia, H.; Jiang, C.; Zuofei, Y.; Wei, W. Microtremor-based analysis of the dynamic response characteristics of earth-fissured sites in the Datong basin, China. *Earthq. Eng. Eng. Vib.* **2021**, *20*, 567–582. [[CrossRef](#)]
31. Cao, G.; Deng, Y.; Chang, J.; Xuan, Y.; He, N.; Mu, H. Dynamic Effect of the Earth Fissure Sites in the Yuncheng Basin, China. *Appl. Sci.* **2023**, *13*, 9923. [[CrossRef](#)]
32. Huang, N.E.; Shen, Z.; Long, S.R.; Wu, M.C.; Shih, H.H.; Zheng, Q.; Yen, N.-C.; Tung, C.C.; Liu, H.H. The empirical mode decomposition and the Hilbert spectrum for nonlinear and non-stationary time series analysis. *Proc. R. Soc. Lond.* **1998**, *454*, 903–995. [[CrossRef](#)]
33. Duan, S.Q.; He, Z.H.; Huang, D.J. Application of the Hilbert-Huang transform to the analysis of seismic signal. *J.-Chengdu Univ. Technol.* **2005**, *32*, 396–400. [[CrossRef](#)]
34. Yinfeng, D.; Yingmin, L.; Mingkui, X.; Ming, L. Analysis of earthquake ground motions using an improved Hilbert–Huang transform. *Soil Dyn. Earthq. Eng.* **2008**, *28*, 7–19. [[CrossRef](#)]
35. Gong, M.S.; Xie, L.L. Discussion on the application of HHT method to earthquake engineering. *World Earthq. Eng.* **2003**, *19*, 39–43. [[CrossRef](#)]
36. Wu, C.; Zhou, R.Z. Application of Hilbert-Huang transform in extracting dynamic properties of seismic signals. *Earthq. Eng. Eng. Vib.* **2006**, *26*, 41–46. [[CrossRef](#)]
37. Peng, Z.; Tse, P.W.; Chu, F. A comparison study of improved Hilbert–Huang transform and wavelet transform: Application to fault diagnosis for rolling bearing. *Mech. Syst. Signal Process.* **2005**, *19*, 974–988. [[CrossRef](#)]
38. Rai, V.K.; Mohanty, A.R. Bearing fault diagnosis using FFT of intrinsic mode functions in Hilbert–Huang transform. *Mech. Syst. Signal Process.* **2007**, *21*, 2607–2615. [[CrossRef](#)]
39. Ahmed, U.; Ali, F.; Jennions, I. A review of aircraft auxiliary power unit faults, diagnostics and acoustic measurements. *Prog. Aerosp. Sci.* **2021**, *124*, 100721. [[CrossRef](#)]
40. Wang, G.Y.; Yu, J.; Wu, S.L.; Wu, J.Q. Land subsidence and compression of soil layers in Changzhou area. *Geol. Explor.* **2009**, *45*, 612–620.
41. Chen, J.; Wang, L.; Wang, P.; Che, A. Failure mechanism investigation on loess–mudstone landslides based on the Hilbert–Huang transform method using a large-scale shaking table test. *Eng. Geol.* **2022**, *302*, 106630. [[CrossRef](#)]
42. Garcia, S.; Romo, M.; Alcántara, L. Analysis of non-linear and non-stationary seismic recordings of Mexico city. *Soil Dyn. Earthq. Eng.* **2019**, *127*, 105859. [[CrossRef](#)]
43. Garcia, S.; Alcántara, L. Empirical decomposition of seismic response of soft soils. *Soil Dyn. Earthq. Eng.* **2019**, *129*, 105918. [[CrossRef](#)]

Disclaimer/Publisher's Note: The statements, opinions and data contained in all publications are solely those of the individual author(s) and contributor(s) and not of MDPI and/or the editor(s). MDPI and/or the editor(s) disclaim responsibility for any injury to people or property resulting from any ideas, methods, instructions or products referred to in the content.